The balance between adaptive and apoptotic unfolded protein responses regulates β-cell death under ER stress conditions through XBP1, CHOP and JNK

Jeng Yie Chan, Jude Luzuriaga, Emma L. Maxwell, Phillip K. West, Mohammed Bensellam and D. Ross Laybutt

From the Garvan Institute of Medical Research, St Vincent's Hospital, University of NSW, Sydney, NSW, Australia

Running title: Balance of the UPR regulates β-cell death

Corresponding Author:

D. Ross Laybutt, Ph.D.

Garvan Institute of Medical Research

384 Victoria St, Darlinghurst, NSW 2010, Australia.

Tel: 61-2-9295-8228

Fax: 61-2-9295-8201

Email: r.laybutt@garvan.org.au

Word count: 3889

Number of figures: 8

Abstract

Endoplasmic reticulum (ER) stress has been implicated in pancreatic β-cell apoptosis in type 1 and type 2 diabetes, although the mechanisms are poorly understood. Here, we show that the balance between XBP1-mediated adaptive unfolded protein response (UPR) and CHOP-dependent apoptotic UPR is critically important for β-cell survival during ER stress. XBP1 inhibition potentiated apoptosis induced by pro-inflammatory cytokines or the saturated fatty acid palmitate in MIN6 β-cells. This response was prevented by CHOP inhibition. XBP1 expression increased with time in islets from diabetes-resistant *ob/ob* mice, but declined in diabetes-prone *db/db* mice. IRE1/XBP1 inhibition led to alterations in islets from *ob/ob* mice that resemble those found in diabetes, including increases in inflammation and antioxidant gene expression and apoptosis. Similarly, IRE1/XBP1 inhibition increased apoptosis in islets from NOD mice. On the other hand, JNK inhibition: 1) increased XBP1 and adaptive UPR gene expression in islets from diabetic *db/db* mice, and 2) restored the adaptive UPR while protecting against pro-apoptotic UPR gene expression and apoptosis following cytokine exposure. The differential regulation of adaptive and apoptotic UPR by JNK provides a mechanism for β-cell propensity to apoptosis rather than ER stress adaptation in type 1 and type 2 diabetes.

The loss of β-cell mass is critical to the development of both type 1 and type 2 diabetes (1). However, the triggering stimuli and the cellular mechanisms involved are poorly understood. Elevated plasma levels of pro-inflammatory cytokines and free fatty acids have been observed in type 1 and type 2 diabetes, and have been proposed as key contributors to β-cell apoptosis (2-4). Indeed, exposure of β-cells to pro-inflammatory cytokines or saturated fatty acids *in vitro* induces apoptosis along with the activation of multiple signaling networks, including endoplasmic reticulum (ER) stress (5-7).

β-cells depend heavily on an efficient ER function due to their high rate of insulin synthesis and secretion. Cytokines and saturated fatty acids have been shown to impair ER homeostasis by inducing depletion of ER Ca^{2+} and alteration of chaperone function, proinsulin processing and ER-Golgi trafficking, and thereby accumulation of misfolded proteins and ER stress (5,8-11). ER stress and its ensuing unfolded protein response (UPR) have been implicated in β-cell pathophysiology in both forms of diabetes (6,12). Recent developments suggest that the induction of ER stress by itself is not a direct cause of β-cell death. The latter instead depends on the inability of the adaptive UPR to cope with the stress (13,14).

The UPR aims at the restoration of ER homeostasis via the ER stress sensors PKR-like ER kinase (PERK), inositol-requiring kinase (IRE) 1, and activating transcription factor (ATF) 6. Activation of PERK and subsequent phosphorylation of the eukaryotic translation initiation factor (eIF) 2α leads to a rapid and transient reduction of global protein translation to reduce ER load (15). Meanwhile, there is a paradoxical increase in the translation of some rare transcripts including the transcription factor ATF4 (16), which regulates the expression of a wide array of

genes implicated in protein folding, metabolism, nutrient uptake, antioxidant response and apoptosis (17). Activation of the endoribonuclease IRE1 results in the unconventional splicing of X-box binding protein 1 (*Xbp1*) mRNA and increased translation of active XBP1 transcription factor (18,19). ATF6 is activated by proteolytic cleavage in the Golgi to release an active transcription factor (20). Together with XBP1, they stimulate the expression of chaperones and ER-associated degradation (ERAD) machinery to enhance ER folding capacity and clearance of misfolded proteins. However, under prolonged or irresolvable ER stress, the UPR switches from an adaptive to an apoptotic role involving different effectors that are yet to be fully identified. The most widely implicated pro-apoptotic UPR effector is the CCAAT/Enhancer-binding Protein Homologous Protein (CHOP), induced downstream of ATF4 (21). CHOP is induced in β-cells following exposure to elevated levels of cytokines (5,22) and saturated fatty acids (6,23) and its inhibition has been shown to improve β-cell survival *in vitro* and *in vivo* (24,25).

Here, we investigated the contribution of two key regulators of adaptive and apoptotic UPR—XBP1 and CHOP to β-cell death in the settings of type 1 and type 2 diabetes. We found that the balance between these transcription factors is critically important in the regulation of β-cell survival. Furthermore, our studies identified JNK as a master regulator of the overall pattern of adaptive and apoptotic UPR gene expression in β-cells.

RESEARCH DESIGN AND METHODS

Cell culture and treatments. The mouse insulinoma cell line MIN6 was maintained in DMEM (Invitrogen, Carlsbad, CA, USA) containing 25 mmol/l glucose, 10 mmol/l HEPES, 10% FCS, 100 U/ml penicillin and 100 μg/ml streptomycin. Either 2 x 10^5 or 8 x 10^5 cells were seeded per

well in a 24-well or 6-well plate, respectively. Cells were treated with 100 U/ml IL-1β, 250 U/ml IFN-γ and 100 U/ml TNF-α (R&D Systems, Minneapolis, MN, USA); 0.92% BSA or 0.4 mmol/l palmitate coupled to 0.92% BSA. 4μ8c (15 μmol/l; Tocris Biosciences, Bristol, UK), and JNK inhibitor II (JNKi, 20 μmol/l SP600125; Merck, Kilsyth, VIC, Australia) were used to inhibit XBP1 and JNK activations, respectively.

Islet isolation and culture. Nonobese diabetic (NOD) and Balb/c mice, and C57BL/KsJ *db/db* and C57BL/6J *ob/ob* mice and their respective lean control mice (C57BL/KsJ or C57BL/6J) were taken from the Garvan Institute breeding colonies. Pancreatic islets were isolated by liberase digestion (Roche Diagnostics, Castle Hill, Australia), gradient centrifugation (Ficoll-Paque PLUS gradient, GE Healthcare Bio-Sciences, Uppsala, Sweden) and handpicking under a stereomicroscope. Procedures were approved by the Garvan Institute/St.Vincent's Hospital Animal Experimentation Ethics Committee, following guidelines issued by the National Health and Medical Research Council of Australia. Islets were cultured at 37 °C in RPMI 1640 medium supplemented with 0.2 mmol/l glutamine, 10% heat-inactivated fetal bovine serum, 100 U/ml penicillin and 100 μg/ml streptomycin. Islets were treated with 100 U/ml IL-1β, 250 U/ml IFN-γ and 100 U/ml TNF-α (R&D Systems) for 24 hours. 4μ8c (15 μmol/l; Tocris Biosciences), and JNK inhibitor II (JNKi, 20 μmol/l SP600125; Merck) were used to inhibit XBP1 and JNK activations, respectively.

Cell death assay. Cell death was determined with the use of a Cell Death Detection ELISA (Roche Diagnostics), which quantifies cytoplasmic histone-associated-DNA-fragments. Islets or cells were lysed in either 0.2 or 0.5 ml of the lysis buffer provided for 30 min at room

temperature. Lysates were then spun at 200xg for 10 min before the ELISA was carried out according to manufacturers' instructions.

Western blotting. Western blotting was performed as previously described (26). The following antibodies were used (1:1000 dilution unless otherwise indicated): CHOP (sc-575) and XBP1 (sc-7160) (Santa Cruz Biotechnology, Santa Cruz, CA, USA); phospho-c-JUN (9164), phospho-JNK (Thr183/Tyr185, 9251), and total JNK (9252) (Cell Signaling Technology, Danvers, MA, USA); and α-tubulin (1:5000; Sigma-Aldrich, St. Louise, MO, USA)).

Real-time RT-PCR. cDNA was synthesised using the QuantiTect Reverse Transcription Kit (Qiagen, Victoria, Australia) according to manufacturer's instructions. Real-time PCR was performed using *Power* SYBR Green PCR Master Mix (Applied Biosystems, Foster City, CA, USA) on a 7900HT Real-Time PCR System (Applied Biosystems). Primer sequences are provided in Supplementary Table 1. The value obtained for each specific product was normalized to a control gene (cyclophilin A) and expressed as a fold-change of the value in control extracts.

***Xbp1* splicing.** *Xbp1* cDNA was amplified by PCR and digested with *Pst*I (New England Biolabs, Ipswitch, MA, USA), which cuts unprocessed *Xbp1* cDNA into fragments. Processed (activated) *Xbp1* cDNA lacks the restriction site and remains intact. Processed (intact) and unprocessed (cut) *Xbp1* were separated using agarose gels and quantified by densitometry. The value obtained for processed *Xbp1* was expressed as a ratio of the total (processed + unprocessed) *Xbp1* mRNA level for each sample. These ratios are expressed as fold-change of the ratio compared to control.

Statistical analysis. All results are presented as means±SEM. Statistical analyses were performed using two-tailed Student's *t* test or ANOVA.

RESULTS

IRE1/XBP1 inhibition potentiates cytokine-induced β-cell death. We first investigated the influence of IRE1/XBP1 signaling on the ER stress response induced by pro-inflammatory cytokines. In MIN6 β-cells, exposure to the combination of cytokines (IL-1β + TNF-α + IFN-γ) for 24 h led to an atypical pattern of UPR activation. Expression of adaptive UPR genes including *Xbp1* (Fig. 1A), *Bip* (Fig. 1C), *Erp72* (Fig. 1D), *Fkbp11* (Fig. 1E), *Grp94* (Fig. 1F) and *Edem1* (Fig. 1G) were reduced after cytokine exposure, whereas expression of pro-apoptotic UPR genes, *Chop* (Fig. 1H) and *Trib3* (Fig. 1I) were increased. In addition, XBP1 activation, as measured by the level of its splicing, was significantly reduced by cytokines (Fig. 1B). This widespread cytokine-mediated alteration in the pattern of UPR gene expression was associated with an increased level of cell death ($p<0.001$, Fig. 1J). Treatment of MIN6 cells with 4μ8c, an IRE1/XBP1 inhibitor, lowered expression of adaptive UPR genes and *Xbp1* splicing (Fig. 1A-G), but did not alter the expression of the pro-apoptotic UPR genes *Chop* (Fig. 1H) and *Trib3* (Fig. 1I). The decline in the adaptive UPR induced by 4μ8c treatment was associated with increased cell death in both control- and cytokine-treated β-cells (Fig. 1J). These results demonstrate the importance of XBP1 and the adaptive UPR in β-cell survival under conditions of cytokine-induced ER stress. In agreement with our findings in MIN6 cells, cytokine-induced cell death was potentiated in mouse islets that were treated with cytokines + 4μ8c as compared to islets treated with cytokines alone (Fig. 1K).

The balance between XBP1-mediated adaptive UPR and CHOP-dependent apoptosis regulates cytokine-induced β-cell death. We next investigated the mechanisms whereby inhibition of XBP1 potentiates cytokine-induced β-cell death using siRNA-mediated knockdown of XBP1 and CHOP in MIN6 cells. In both control- and cytokine-treated cells, siXBP1 transfection significantly reduced XBP1 protein (Fig. 2A) and mRNA (Fig. 2C) levels. This was associated with the widespread downregulation of adaptive UPR genes (Fig. 2D-H), whereas CHOP levels were similar to control (Fig. 2A, I). *Trib3* (Fig. 2J) mRNA levels were slightly reduced by siXBP1 in cytokine-treated cells. These changes in gene expression induced by siXBP1 were associated with increased cell death in control- and cytokine-treated cells (Fig. 2B). The increase in β-cell death after XBP1 inhibition could not be attributed to enhanced JNK activity (Fig. 2A). In contrast, the siXBP1-mediated increase in cell death was completely abolished when cells were co-transfected with siCHOP (Fig. 2B). Co-transfection with siCHOP significantly reduced the expression of CHOP (Fig. 2A, I) without affecting the expression of XBP1 (Fig. 2A, C) and other adaptive UPR genes (Fig. 2D-H) or JNK phosphorylation (Fig. 2A). These data indicate that CHOP expression is required for the siXBP1-mediated increase in both control and cytokine-induced β-cell death. Interestingly, this occurs despite unchanged CHOP levels in XBP1-deficient cells. Thus, the findings suggest that the balance between XBP1-mediated adaptive UPR and CHOP-dependent apoptosis is critically important for β-cell survival.

The balance between XBP1-mediated adaptive UPR and CHOP-dependent apoptosis regulates palmitate-induced β-cell death. We investigated the influence of XBP1 and CHOP on MIN6 β-cell apoptosis in the context of lipotoxicity and ER stress induced by the saturated

fatty acid palmitate. In contrast to cytokines, palmitate treatment increased the expression of *Xbp1* mRNA (Fig. 3C) and the associated adaptive UPR genes (Fig. 3D-G), with the exception of *Edem1* (Fig. 3H). Expression of CHOP (Fig. 3A, I) and *Trib3* (Fig. 3J) were also increased by palmitate exposure. Collectively, these gene expression changes induced by palmitate were associated with a significant increase in cell death ($p<0.001$, Fig. 3B). MIN6 cells transfected with siXBP1 displayed reduced levels of XBP1 mRNA (Fig. 3C) and protein (Fig. 3A), accompanied by decreases in the other adaptive UPR genes (Fig. 3D-H). *Chop* (Fig. 3I) and *Trib3* (Fig. 3J) mRNA levels were slightly reduced by XBP1 silencing following palmitate exposure. Interestingly, XBP1 knockdown significantly increased cell death in both control- and palmitate-treated MIN6 cells (Fig. 3B). This increase in cell death was not associated with changes in JNK phosphorylation (Fig. 3A), but was completely prevented by the co-transfection of cells with siCHOP (Fig. 3B). Co-transfection with siCHOP lowered CHOP protein and mRNA levels (Fig. 3A, I), but did not affect other UPR genes (Fig. 3D-H). These results suggest that the maintenance of the adaptive UPR by XBP1 inhibits CHOP-dependent apoptosis under conditions of palmitate-induced ER stress. The observations confirm the suggestion that the balance between XBP1 and CHOP activities, rather than their expression levels *per se*, is critically important in the regulation of β-cell survival.

IRE1/XBP1 inhibition increases apoptosis in islets from NOD mice. Recent studies suggest that β-cell ER stress precedes the onset of type 1 diabetes in the NOD mouse model (27,28), and that progressive loss of adaptive UPR mediators, including XBP1, occurs as the disease progresses (22,28). To assess the influence of XBP1 expression on β-cell survival prior to the onset of type 1 diabetes in this model, islets were isolated from 5-6 week-old NOD mice and

treated with the IRE1/XBP1 inhibitor, 4μ8c. NOD islets displayed reduced *Xbp1* splicing (Fig. 4B), *Erp72* (Fig. 4D) and *Fkbp11* (Fig. 4E) expression, whereas total *Xbp1* (Fig. 4A), *Bip* (Fig. 4C), *Grp94* (Fig. 4F) and *Edem1* (Fig. 4G) expression levels were similar to control islets. *Chop* mRNA expression (Fig. 4H) along with cell death (Fig. 4J) were increased in NOD islets. Treatment of NOD islets with 4μ8c led to significant decreases in *Xbp1* expression (Fig. 4A) and splicing (Fig. 4B). Along with a widespread downregulation of adaptive UPR genes (Fig. 4C-G), *Chop* (Fig. 4H) and *Trib3* (Fig. 4I) mRNA levels were increased. Strikingly, this altered pattern of UPR gene expression was associated with increased cell death in 4μ8c-treated NOD islets compared to control NOD islets (Fig. 4J). These results suggest that XBP1-mediated adaptive UPR protects against pro-apoptotic UPR gene expression (*Chop* and *Trib3*) and apoptosis in NOD islets prior to the onset of type 1 diabetes.

IRE1/XBP1 inhibition increases apoptosis in islets from obese diabetes-resistant *ob/ob* mice. The *db/db* and *ob/ob* mouse models of obesity exhibit opposing disposition to diabetes development (29). The *ob/ob* mouse displays resistance to diabetes due to successful β-cell compensation, whereas the *db/db* mouse displays time-dependent progression to overt diabetes due to the failure of β-cell compensation. We previously reported that the mRNA levels of adaptive UPR genes were progressively increased in islets of diabetes-resistant *ob/ob* mice, whereas they declined in diabetic *db/db* mice (29). Here, we show that the status of the adaptive UPR in these models correlates with *Xbp1* expression; *Xbp1* mRNA expression displayed a time-dependent increase in islets of *ob/ob* mice, whereas it declined in diabetic *db/db* islets (Supp Fig. 1). We investigated the role of *Xbp1* expression in islets of diabetes-resistant *ob/ob* mice using *ex vivo* treatment with 4μ8c. In comparison to untreated *ob/ob* islets, 4μ8c treatment markedly

reduced the levels of *Xbp1* mRNA (Fig. 5A) and splicing (Fig. 5B). mRNA levels of other adaptive UPR genes were downregulated (Fig. 5C-G), whereas *Chop* (Fig. 5H) and *Trib3* (Fig. 5I) were increased. Similar to findings with NOD mouse islets, treatment of *ob/ob* islets with 4μ8c led to increased cell death compared to control-treated *ob/ob* islets (Fig. 5J). These findings suggest that XBP1 protects against deleterious UPR signaling and apoptosis in the *ob/ob* mouse model of β-cell compensation.

A notable difference in the gene expression profiles of *db/db* and *ob/ob* islets is the preferential upregulation of antioxidant and inflammation genes in islets of diabetes-prone *db/db* mice (29). Here, we assessed the influence of IRE1/XBP1 activity on antioxidant and inflammatory gene expression in *ob/ob* islets. Glutathione peroxidase (*GPx*) (Fig. 6C), *IL-6* (Fig. 6G), *Ccl2* (Fig. 6H), and the death receptor *Fas* (Fig. 6E) mRNA levels were similar in islets from *ob/ob* mice compared to control islets, whereas catalase (Fig. 6A), heme oxygenase-1 (*HO-1*) (Fig. 6B), *IL-1β* (Fig. 6F), and *Cxcl1* (Fig. 6I) mRNA levels were slightly increased. Interestingly, inhibition of IRE1/XBP1 with 4μ8c treatment led to significant increases in the expression of each of these antioxidant and inflammation genes in *ob/ob* islets (Fig. 6A-I). Superoxide dismutase 1 (*Sod1*) displayed a tendency ($p<0.08$) towards an increased expression in 4μ8c-treated *ob/ob* islets compared to untreated *ob/ob* islets (Fig. 6D). These results suggest for the first time that the IRE1/XBP1-mediated adaptive UPR protects against islet inflammation and oxidative stress in the *ob/ob* mouse model of β-cell compensation. Taken together with previous findings (29). our results suggest that IRE1/XBP1 inhibition leads to alterations in islets from *ob/ob* mice that resemble those found in the *db/db* model of β-cell failure and diabetes, namely declining adaptive UPR gene expression, increased apoptosis and marked upregulation of antioxidant and

inflammatory genes. Thus, our findings suggest that XBP1 may play a key role in the maintenance of β-cell compensation and protection against type 2 diabetes under conditions of obesity-associated ER stress.

JNK activity differentially regulates adaptive and apoptotic UPR in β-cells. Having established the importance of the balance between adaptive and apoptotic UPR in β-cell survival in models of ER stress and type 1 and type 2 diabetes, we next tested whether JNK activity influences the UPR. JNK and c-JUN phosphorylation were markedly increased in cytokine-treated MIN6 cells (Fig. 7A) in association with reduced adaptive and increased apoptotic UPR gene expression (Fig. 7C-K). In cells treated with JNKi, cytokine-mediated JNK and c-JUN phosphorylation were reduced (Fig. 7A). Inhibition of JNK activity completely protected against the cytokine-mediated reductions in adaptive UPR gene expression (Fig 7E-I). Furthermore, the cytokine-mediated increases in CHOP (Fig. 7 A, J), *Trib3* (Fig. 7K) and β-cell death (Fig. 7B) were partially prevented by JNK inhibition. These data indicate that JNK signaling is necessary for alterations in the general UPR gene expression pattern in cytokine-treated β-cells. JNK activation contributes to the downregulation of XBP1 and adaptive UPR while promoting apoptotic UPR gene expression in cytokine-stimulated β-cells. Thus, our findings implicate JNK as a master regulator of the nature of UPR under conditions of immune-mediated ER stress and type 1 diabetes.

JNK inhibition increases adaptive UPR gene expression in *db/db* mouse islets. We also assessed the influence of JNK activation in the decline of adaptive UPR gene expression in islets of diabetic *db/db* mice. Islets were isolated from diabetic *db/db* mice and cultured in the absence

or presence of JNKi. Inhibition of JNK significantly increased both the mRNA levels and splicing of *Xbp1* (Fig. 8A, B). Furthermore, JNK inhibition increased the mRNA levels of the adaptive UPR genes *Bip* (Fig. 8C), *Erp72* (Fig. 8D), *Fkbp11* (Fig. 8E), *Grp94* (Fig. 8F) and *Edem1* (Fig. 8G), whereas *Chop* (Fig. 8H) and *Trib3* (Fig. 8I) mRNA levels were similar among the groups. These findings suggest that JNK signaling contributes to the decline of adaptive UPR gene expression in islets of diabetic *db/db* mice. Thus, similar to immune-mediated ER stress and type 1 diabetes above, JNK activation may regulate the pattern of UPR gene expression under conditions of obesity-associated ER stress and type 2 diabetes.

DISCUSSION

Even though ER stress has long been implicated in β-cell death in type 1 (12,27) and type 2 diabetes (6,14,24,30,31), the precise mechanisms are understudied. Growing evidence supports the concept that a complex fine-tuning of the UPR is crucial for the maintenance of β-cell mass under physiological and pathological situations (13,14). Indeed, reduced XBP1 and adaptive UPR gene expression has been shown to correlate with increased β-cell apoptosis and the onset of diabetes (22,28). On the other hand, deletion of CHOP has been shown to correlate with reduced β-cell apoptosis and delayed onset of diabetes (24,30). Our studies suggest that the balance between XBP1 and CHOP activation is critically important in the regulation of β-cell survival. Thus, the interaction between XBP1-mediated adaptive UPR and CHOP-dependent apoptosis determines β-cell fate following cytokine or saturated fatty acid exposure. Moreover, our studies suggest that JNK acts as a master regulator of the general pattern of adaptive and apoptotic UPR gene expression under conditions of inflammatory- and obesity-associated ER stress.

The activation of the PERK-ATF4-CHOP arm of the UPR by pro-inflammatory cytokines has received much attention because of the important and well-established role of CHOP in apoptosis, whereas the IRE1-XBP1 arm has received less attention (5,8,22,32). In the present study, we have shown that cytokine treatment increased *Chop* and *Trib3* expression and β-cell apoptosis whilst inducing a global attenuation of the IRE1-XBP1 arm of the UPR. This observation is in good agreement with previous studies in NOD mice showing a progressive decline in the expression of XBP1, ATF6 and several chaperones between pre-diabetic and diabetic stages (22,28). Interestingly, the inhibition of IRE1 reduced XBP1 splicing and downstream chaperone expression along with a marked potentiation of apoptosis in the absence of any change in the expression of *Chop*. These effects on survival were reproduced by *Xbp1* silencing and prevented by the co-silencing of *Chop*. These findings introduce a novel concept to the field by showing that the decrease in XBP1-dependent adaptive UPR alone can trigger β-cell death without necessarily increasing the expression of apoptotic UPR genes. Our current findings suggest that a balance between the two, rather than a direct increase in either, is critically important in the regulation of β-cell survival.

Contrary to previous reports claiming that the loss of XBP1 affects lipid- but not cytokine-induced β-cell death (33,34), this current study showed that a relative XBP1:CHOP deficiency is a strong inducer of β-cell death in both settings. Our results also contrast with a recent report showing that IRE1 inhibition in INS1 cells expressing mutated insulin, although slightly altered the expression of some chaperones, did not sensitize these cells to ER stress-induced apoptosis (35). These differences may be attributed to the use of different experimental models, species

and timing of experiments. In addition, because of the importance of the XBP1:CHOP balance in β-cell death, there is an additional level of complexity that was not investigated in these models. Thus, the differential effects reported by previous studies could be due to differential expression of CHOP in the experimental models.

In further evidence, inhibition of IRE1 in isolated islets from pre-diabetic NOD and diabetes-resistant *ob/ob* mice led to an attenuated *Xbp1* expression and splicing, accompanied by decreases in expression of chaperone and ERAD genes. Meanwhile, *Chop* and *Trib3* mRNA levels were markedly increased by the treatment. These changes were accompanied by increased apoptosis, thereby reinforcing the importance of XBP:CHOP ratio in the regulation of β-cell survival.

In addition to CHOP, IRE1 has also been implicated in ER stress-induced β-cell apoptosis and loss of differentiation via the activation of JNK, caspase 12 and degradation of ER-associated mRNAs, including proinsulin mRNA (32,36-39). JNK activation has been implicated in β-cell apoptosis after cytokine treatment via yet to be fully-identified mechanisms (26,40-42). Interestingly, the expression of DP5, a protein important in cytokine- and lipid-mediated β-cell death during ER stress (43,44), is regulated by a JNK-dependent transcription factor c-JUN (21). Besides, we have previously reported that JNK plays an important role in the activation of CHOP downstream of nitric oxide (26). Therefore, JNK is a potential interesting target to modulate the XBP1:CHOP balance under ER stress towards the improvement of β-cell survival in the settings of type 1 and type 2 diabetes. Indeed, JNK inhibition partially protected against cytokine-induced β-cell death while restoring XBP1:CHOP balance. Our current study shows for the first

time that, rather than directly activating pro-apoptotic UPR, JNK plays a role in the regulation of XBP1:CHOP balance, thereby controlling β-cell survival in response to inflammatory- and obesity-associated ER stress.

Further to our previous report showing that β-cell decompensation in *db/db* mice and loss of the adaptive UPR was accompanied by increased islet expression of oxidative stress and inflammation genes (29), this study demonstrated that the inhibition of IRE1/XBP1 in islets of a model of successful β-cell compensation was sufficient to trigger at least some of these changes. This supports the notion that ER stress and adaptive UPR may be an early event that precedes oxidative stress and inflammation in the progression to β-cell failure. Indeed, disruption of adaptive UPR signaling has been shown to induce accumulation of unfolded proteins in the ER and generation of reactive oxygen species (45). Moreover, ER stress has been shown to activate the inflammasome and subsequent β-cell death through the activation of thioredoxin-interacting protein (46).

In conclusion, our studies show that: 1) XBP1 is a crucial regulator of the adaptive UPR and β-cell survival in models of type 1 and type 2 diabetes, 2) the balance between XBP1-mediated adaptive UPR and CHOP-dependent apoptosis determines β-cell fate during ER stress, and 3) JNK acts as a master regulator of the global pattern of UPR gene expression by downregulating XBP1 and the adaptive UPR while promoting apoptotic ER stress signaling. These observations reveal important molecular mechanisms governing β-cell survival during ER stress and support the growing interest in targeting ER function for the treatment of both type 1 and type 2 diabetes (28,47-49).

ACKNOWLEDGEMENTS

This work was supported by a grant from the National Health and Medical Research Council (NHMRC) of Australia. D.R.L. is supported by an Australian Research Council (ARC) Future Fellowship.

The authors declare no conflicts of interest relevant to this article.

REFERENCES

1. Matveyenko AV, Butler PC. Relationship between beta-cell mass and diabetes onset. Diabetes Obes Metab 2008;10 Suppl 4:23-31

2. Cnop M, Welsh N, Jonas JC, Jorns A, Lenzen S, Eizirik DL. Mechanisms of pancreatic beta-cell death in type 1 and type 2 diabetes: many differences, few similarities. Diabetes 2005;54:S97-S107

3. Biden TJ, Boslem E, Chu KY, Sue N. Lipotoxic endoplasmic reticulum stress, beta cell failure, and type 2 diabetes mellitus. Trends Endocrinol Metab 2014;25:389-398

4. Donath MY, Shoelson SE. Type 2 diabetes as an inflammatory disease. Nat Rev Immunol 2011;11:98-107

5. Cardozo AK, Ortis F, Storling J, Feng YM, Rasschaert J, Tonnesen M, Van Eylen F, Mandrup-Poulsen T, Herchuelz A, Eizirik DL. Cytokines downregulate the sarcoendoplasmic reticulum pump Ca2+ ATPase 2b and deplete endoplasmic reticulum Ca2+, leading to induction of endoplasmic reticulum stress in pancreatic beta-cells. Diabetes 2005;54:452-461

6. Laybutt DR, Preston AM, Akerfeldt MC, Kench JG, Busch AK, Biankin AV, Biden TJ. Endoplasmic reticulum stress contributes to beta cell apoptosis in type 2 diabetes. Diabetologia 2007;50:752-763

7. Cunha DA, Hekerman P, Ladriere L, Bazarra-Castro A, Ortis F, Wakeham MC, Moore F, Rasschaert J, Cardozo AK, Bellomo E, Overbergh L, Mathieu C, Lupi R, Hai T, Herchuelz A, Marchetti P, Rutter GA, Eizirik DL, Cnop M. Initiation and execution of lipotoxic ER stress in pancreatic beta-cells. J Cell Sci 2008;121:2308-2318

8. Oyadomari S, Takeda K, Takiguchi M, Gotoh T, Matsumoto M, Wada I, Akira S, Araki E, Mori M. Nitric oxide-induced apoptosis in pancreatic beta cells is mediated by the endoplasmic reticulum stress pathway. Proc Natl Acad Sci U S A 2001;98:10845-10850

9. Preston AM, Gurisik E, Bartley C, Laybutt DR, Biden TJ. Reduced endoplasmic reticulum (ER)-to-Golgi protein trafficking contributes to ER stress in lipotoxic mouse beta cells by promoting protein overload. Diabetologia 2009;52:2369-2373

10. Hara T, Mahadevan J, Kanekura K, Hara M, Lu S, Urano F. Calcium efflux from the endoplasmic reticulum leads to beta-cell death. Endocrinology 2014;155:758-768

11. Jeffrey KD, Alejandro EU, Luciani DS, Kalynyak TB, Hu X, Li H, Lin Y, Townsend RR, Polonsky KS, Johnson JD. Carboxypeptidase E mediates palmitate-induced beta-cell ER stress and apoptosis. Proc Natl Acad Sci U S A 2008;105:8452-8457

12. Marhfour I, Lopez XM, Lefkaditis D, Salmon I, Allagnat F, Richardson SJ, Morgan NG, Eizirik DL. Expression of endoplasmic reticulum stress markers in the islets of patients with type 1 diabetes. Diabetologia 2012;55:2417-2420

13. Fonseca SG, Gromada J, Urano F. Endoplasmic reticulum stress and pancreatic beta-cell death. Trends Endocrinol Metab 2011;22:266-274

14. Scheuner D, Kaufman RJ. The unfolded protein response: a pathway that links insulin demand with beta-cell failure and diabetes. Endocr Rev 2008;29:317-333

15. Harding HP, Zhang Y, Ron D. Protein translation and folding are coupled by an endoplasmic-reticulum-resident kinase. Nature 1999;397:271-274

16. Lu PD, Harding HP, Ron D. Translation reinitiation at alternative open reading frames regulates gene expression in an integrated stress response. J Cell Biol 2004;167:27-33

17. Schroder M, Kaufman RJ. The mammalian unfolded protein response. Annu Rev Biochem 2005;74:739-789

18. Lee AH, Heidtman K, Hotamisligil GS, Glimcher LH. Dual and opposing roles of the unfolded protein response regulated by IRE1alpha and XBP1 in proinsulin processing and insulin secretion. Proc Natl Acad Sci U S A 2011;108:8885-8890

19. Yoshida H, Matsui T, Hosokawa N, Kaufman RJ, Nagata K, Mori K. A time-dependent phase shift in the mammalian unfolded protein response. Dev Cell 2003;4:265-271

20. Haze K, Yoshida H, Yanagi H, Yura T, Mori K. Mammalian transcription factor ATF6 is synthesized as a transmembrane protein and activated by proteolysis in response to endoplasmic reticulum stress. Mol Biol Cell 1999;10:3787-3799

21. Ma Y, Brewer JW, Diehl JA, Hendershot LM. Two distinct stress signaling pathways converge upon the CHOP promoter during the mammalian unfolded protein response. J Mol Biol 2002;318:1351-1365

22. Akerfeldt MC, Howes J, Chan JY, Stevens VA, Boubenna N, McGuire HM, King C, Biden TJ, Laybutt DR. Cytokine-induced beta-cell death is independent of endoplasmic reticulum stress signaling. Diabetes 2008;57:3034-3044

23. Karaskov E, Scott C, Zhang L, Teodoro T, Ravazzola M, Volchuk A. Chronic palmitate but not oleate exposure induces endoplasmic reticulum stress, which may contribute to INS-1 pancreatic beta-cell apoptosis. Endocrinology 2006;147:3398-3407

24. Song B, Scheuner D, Ron D, Pennathur S, Kaufman RJ. Chop deletion reduces oxidative stress, improves beta cell function, and promotes cell survival in multiple mouse models of diabetes. J Clin Invest 2008;118:3378-3389

25. Allagnat F, Fukaya M, Nogueira TC, Delaroche D, Welsh N, Marselli L, Marchetti P, Haefliger JA, Eizirik DL, Cardozo AK. C/EBP homologous protein contributes to cytokine-induced pro-inflammatory responses and apoptosis in beta-cells. Cell Death Differ 2012;19:1836-1846

26. Chan JY, Cooney GJ, Biden TJ, Laybutt DR. Differential regulation of adaptive and apoptotic unfolded protein response signalling by cytokine-induced nitric oxide production in mouse pancreatic beta cells. Diabetologia 2011;54:1766-1776

27. Tersey SA, Nishiki Y, Templin AT, Cabrera SM, Stull ND, Colvin SC, Evans-Molina C, Rickus JL, Maier B, Mirmira RG. Islet beta-cell endoplasmic reticulum stress precedes the onset of type 1 diabetes in the nonobese diabetic mouse model. Diabetes 2012;61:818-827

28. Engin F, Yermalovich A, Nguyen T, Hummasti S, Fu W, Eizirik DL, Mathis D, Hotamisligil GS. Restoration of the unfolded protein response in pancreatic beta cells protects mice against type 1 diabetes. Sci Transl Med 2013;5:211ra156

29. Chan JY, Luzuriaga J, Bensellam M, Biden TJ, Laybutt DR. Failure of the adaptive unfolded protein response in islets of obese mice is linked with abnormalities in beta-cell gene expression and progression to diabetes. Diabetes 2013;62:1557-1568

30. Oyadomari S, Koizumi A, Takeda K, Gotoh T, Akira S, Araki E, Mori M. Targeted disruption of the Chop gene delays endoplasmic reticulum stress-mediated diabetes. J Clin Invest 2002;109:525-532

31. Marchetti P, Bugliani M, Lupi R, Marselli L, Masini M, Boggi U, Filipponi F, Weir GC, Eizirik DL, Cnop M. The endoplasmic reticulum in pancreatic beta cells of type 2 diabetes patients. Diabetologia 2007;50:2486-2494

32. Pirot P, Naamane N, Libert F, Magnusson NE, Orntoft TF, Cardozo AK, Eizirik DL. Global profiling of genes modified by endoplasmic reticulum stress in pancreatic beta cells reveals the early degradation of insulin mRNAs. Diabetologia 2007;50:1006-1014

33. Allagnat F, Christulia F, Ortis F, Pirot P, Lortz S, Lenzen S, Eizirik DL, Cardozo AK. Sustained production of spliced X-box binding protein 1 (XBP1) induces pancreatic beta cell dysfunction and apoptosis. Diabetologia 2010;53:1120-1130

34. Cunha DA, Gurzov EN, Naamane N, Ortis F, Cardozo AK, Bugliani M, Marchetti P, Eizirik DL, Cnop M. JunB protects beta-cells from lipotoxicity via the XBP1-AKT pathway. Cell Death Differ 2014;21:1313-1324

35. Zhang L, Nosak C, Sollazzo P, Odisho T, Volchuk A. IRE1 inhibition perturbs the unfolded protein response in a pancreatic beta-cell line expressing mutant proinsulin, but does not sensitize the cells to apoptosis. BMC Cell Biol 2014;15:29

36. Lipson KL, Ghosh R, Urano F. The role of IRE1alpha in the degradation of insulin mRNA in pancreatic beta-cells. PLoS ONE 2008;3:e1648

37. Han D, Lerner AG, Vande Walle L, Upton JP, Xu W, Hagen A, Backes BJ, Oakes SA, Papa FR. IRE1alpha kinase activation modes control alternate endoribonuclease outputs to determine divergent cell fates. Cell 2009;138:562-575

38. Urano F, Wang X, Bertolotti A, Zhang Y, Chung P, Harding HP, Ron D. Coupling of stress in the ER to activation of JNK protein kinases by transmembrane protein kinase IRE1. Science 2000;287:664-666

39. Yoneda T, Imaizumi K, Oono K, Yui D, Gomi F, Katayama T, Tohyama M. Activation of caspase-12, an endoplastic reticulum (ER) resident caspase, through tumor necrosis factor receptor-associated factor 2-dependent mechanism in response to the ER stress. J Biol Chem 2001;276:13935-13940

40. Bonny C, Oberson A, Negri S, Sauser C, Schorderet DF. Cell-permeable peptide inhibitors of JNK: novel blockers of beta-cell death. Diabetes 2001;50:77-82

41. Brozzi F, Gerlo S, Grieco FA, Nardelli TR, Lievens S, Gysemans C, Marselli L, Marchetti P, Mathieu C, Tavernier J, Eizirik DL. A Combined "Omics" Approach Identifies N-Myc Interactor as a Novel Cytokine-induced Regulator of IRE1alpha Protein and c-Jun N-terminal Kinase in Pancreatic Beta Cells. J Biol Chem 2014;289:20677-20693

42. Marroqui L, Santin I, Dos Santos RS, Marselli L, Marchetti P, Eizirik DL. BACH2, a Candidate Risk Gene for Type 1 Diabetes, Regulates Apoptosis in Pancreatic beta-Cells via JNK1 Modulation and Crosstalk With the Candidate Gene PTPN2. Diabetes 2014;63:2516-2527

43. Gurzov EN, Ortis F, Cunha DA, Gosset G, Li M, Cardozo AK, Eizirik DL. Signaling by IL-1beta+IFN-gamma and ER stress converge on DP5/Hrk activation: a novel mechanism for pancreatic beta-cell apoptosis. Cell Death Differ 2009;16:1539-1550

44. Cunha DA, Igoillo-Esteve M, Gurzov EN, Germano CM, Naamane N, Marhfour I, Fukaya M, Vanderwinden JM, Gysemans C, Mathieu C, Marselli L, Marchetti P, Harding HP, Ron D, Eizirik DL, Cnop M. Death protein 5 and p53-upregulated modulator of apoptosis mediate the

endoplasmic reticulum stress-mitochondrial dialog triggering lipotoxic rodent and human beta-cell apoptosis. Diabetes 2012;61:2763-2775

45. Kaufman RJ, Back SH, Song B, Han J, Hassler J. The unfolded protein response is required to maintain the integrity of the endoplasmic reticulum, prevent oxidative stress and preserve differentiation in beta-cells. Diabetes Obes Metab 2010;12 Suppl 2:99-107

46. Oslowski CM, Hara T, O'Sullivan-Murphy B, Kanekura K, Lu S, Hara M, Ishigaki S, Zhu LJ, Hayashi E, Hui ST, Greiner D, Kaufman RJ, Bortell R, Urano F. Thioredoxin-interacting protein mediates ER stress-induced beta cell death through initiation of the inflammasome. Cell Metab 2012;16:265-273

47. Urano F. Diabetes: Targeting endoplasmic reticulum to combat juvenile diabetes. Nat Rev Endocrinol 2014;10:129-130

48. Engin F, Hotamisligil GS. Restoring endoplasmic reticulum function by chemical chaperones: an emerging therapeutic approach for metabolic diseases. Diabetes Obes Metab 2010;12 Suppl 2:108-115

49. Xiao C, Giacca A, Lewis GF. Sodium phenylbutyrate, a drug with known capacity to reduce endoplasmic reticulum stress, partially alleviates lipid-induced insulin resistance and beta-cell dysfunction in humans. Diabetes 2011;60:918-924

Figure Legends

Figure 1. Effect of IRE1/XBP1 inhibition on cytokine-mediated changes in gene expression and β-cell death. MIN6 cells or isolated mouse islets were incubated in the absence *(white bars)* or presence *(black bars)* of the combination of IL-1β (100U/ml), IFN-γ (250U/ml) and TNF-α (100U/ml) with or without 4μ8c (15μmol/l) as indicated for 24 h. Total RNA was extracted, reverse-transcribed and analyzed by real-time RT-PCR for *Xbp1* (A), *Bip* (C), *Erp72* (D), *Fkbp11* (E), *Grp94* (F), *Edem1* (G), *Chop* (H) and *Trib3* (I). B: *Xbp1* cDNA was amplified by PCR and digested with *Pst*I which cuts unprocessed *Xbp1* into fragments. Processed (activated) *Xbp1* lacks the restriction site and remains intact. Processed (intact) and unprocessed (cut) *Xbp1* were quantified by densitometry. The value obtained for processed *Xbp1* was expressed as a ratio of the total (processed + unprocessed) *Xbp1* mRNA level for each sample. These ratios are expressed as fold-change of the ratio in untreated control. Cell death was determined using a cell death detection ELISA in MIN6 cells (J) and isolated mouse islets (K) and expressed as fold-change compared to untreated control. All results are mean±SEM determined from at least three experiments; *$p<0.05$, **$p<0.01$, ***$p<0.001$ cytokine effect in each group; †$p<0.05$, ††$p<0.01$, †††$p<0.001$ 4μ8c effect in each treatment group.

Figure 2. Effect of siRNA-mediated silencing of XBP1 and CHOP on cytokine-mediated changes in gene expression and β-cell death. MIN6 cells were transfected with either the ON-TARGETplus SMARTpool negative control non-targeting siRNA (*white bars*) or siRNA against XBP1 (*black bars*) or CHOP (*light grey bars*) or against both XBP1 and CHOP (*dark grey bars*) using DharmaFECT Transfection Reagent for 24 h. Cells were then cultured in the absence or

presence of the combination of IL-1β (100U/ml), IFN-γ (250U/ml) and TNF-α (100U/ml) for 6 h. Western blot was performed on protein extracts for JNK phosphorylation (p), XBP1, and CHOP. Total (t) JNK, tubulin served as loading controls (A). Cell death was determined using a cell death detection ELISA in MIN6 cells and expressed as fold-change compared to untreated control (B). Total RNA was extracted, reverse-transcribed and analyzed by real-time RT-PCR for *Xbp1* (C), *Bip* (D), *Erp72* (E), *Fkbp11* (F), *Grp94* (G), *Edem1* (H), *Chop* (I) and *Trib3* (J). All results are mean±SEM determined from at least three experiments; **p*<0.05, ***p*<0.01, ****p*<0.001 versus siControl; †*p*<0.05, ††*p*<0.01, †††*p*<0.001 versus siXBP1.

Figure 3. Effect of siRNA-mediated silencing of XBP1 and CHOP on palmitate-mediated changes in gene expression and β-cell death. MIN6 cells were transfected with either the ON-TARGETplus SMARTpool negative control non-targeting siRNA (*white bars*) or siRNA against XBP1 (*black bars*) or CHOP (*light grey bars*) or against both XBP1 and CHOP (*dark grey bars*) using DharmaFECT Transfection Reagent for 24 h. Cells were then cultured in the presence of 0.92% BSA or 0.4 mmol/l palmitate coupled to 0.92% BSA for 24 h. Western blot was performed on protein extracts for JNK phosphorylation (p), XBP1, and CHOP. Total (t) JNK, tubulin served as loading controls (A). Cell death was determined using a cell death detection ELISA in MIN6 cells and expressed as fold-change compared to untreated control (B). Total RNA was extracted, reverse-transcribed and analyzed by real-time RT-PCR for *Xbp1* (C), *Bip* (D), *Erp72* (E), *Fkbp11* (F), *Grp94* (G), *Edem1* (H), *Chop* (I) and *Trib3* (J). All results are mean±SEM determined from at least three experiments; **p*<0.05, ***p*<0.01, ****p*<0.001 versus siControl; †*p*<0.05, ††*p*<0.01, †††*p*<0.001 versus siXBP1.

Figure 4. Effect of IRE1/XBP1 inhibition on the changes in UPR gene expression and cell death in NOD mouse islets. Islets isolated from female NOD and control mice (5-6 weeks of age) were cultured in the absence (control, *white bars*; and NOD, *black bars*) or presence (NOD, *striped bars*) of IRE1/XBP1 inhibitor (4μ8c, 15 μmol/l) for 40 h. Total RNA was extracted, reverse-transcribed and analyzed by real-time RT-PCR for *Xbp1* (A), *Bip* (C), *Erp72* (D), *Fkbp11* (E), *Grp94* (F), *Edem1* (G), *Chop* (H) and *Trib3* (I). B: *Xbp1* splicing was analyzed and expressed as described in Fig. 1. Cell death was determined using a cell death detection ELISA and expressed as fold-change compared to control (J). All results are mean±SEM determined from at least three experiments; **p*<0.05, ***p*<0.01, ****p*<0.001 genotype effect; †*p*<0.05, ††*p*<0.01, †††*p*<0.001 4μ8c treatment effect in NOD islets.

Figure 5. Effect of IRE1/XBP1 inhibition on the changes in UPR gene expression and cell death in *ob/ob* mouse islets. Islets isolated from *ob/ob* and control mice were cultured in the absence (control, *white bars*; and *ob/ob*, *black bars*) or presence (*ob/ob*, *striped bars*) of IRE1/XBP1 inhibitor (4μ8c, 15 μmol/l) for 40 h. Total RNA was extracted, reverse-transcribed and analyzed by real-time RT-PCR for *Xbp1* (A), *Bip* (C), *Erp72* (D), *Fkbp11* (E), *Grp94* (F), *Edem1* (G), *Chop* (H) and *Trib3* (I). B: *Xbp1* splicing was analyzed and expressed as described in Fig. 1. Cell death was determined using a cell death detection ELISA and expressed as fold-change compared to control (J). All results are mean±SEM determined from at least three experiments; **p*<0.05, ***p*<0.01, ****p*<0.001 genotype effect; †*p*<0.05, ††*p*<0.01, †††*p*<0.001 4μ8c treatment effect in *ob/ob* islets.

Figure 6. Effect of IRE1/XBP1 inhibition on the changes in antioxidant and inflammation gene expression in *ob/ob* mouse islets. Islets isolated from *ob/ob* and control mice were cultured in the absence (control, *white bars*; and *ob/ob*, *black bars*) or presence (*ob/ob*, *striped bars*) of IRE1/XBP1 inhibitor (4μ8c, 15 μmol/l) for 40 h. Total RNA was extracted, reverse-transcribed and analyzed by real-time RT-PCR for *Catalase* (A), *HO-1* (B), *GPx* (C), *Sod1* (D), *Fas* (E), *IL-1β* (F), *IL-6* (G), *Ccl2* (H), and *Cxcl1* (I). All results are mean±SEM determined from at least three experiments; ***p*<0.05, ***p*<0.01, ****p*<0.001 genotype effect; †*p*<0.05, ††*p*<0.01, †††*p*<0.001 4μ8c treatment effect in *ob/ob* islets.

Figure 7. Effect of JNK inhibition on cytokine-mediated changes in gene expression and β-cell death. MIN6 cells were incubated in the absence *(white bars)* or presence *(black bars)* of the combination of IL-1β (100U/ml), IFN-γ (250U/ml) and TNF-α (100U/ml) with or without JNK inhibitor (JNKi, 20μmol/l) as indicated for 24 h. Western blot was performed on protein extracts for JNK and c-JUN phosphorylation (p), XBP1, and CHOP. Total (t) JNK, tubulin served as loading controls (A). Cell death was determined using a cell death detection ELISA in MIN6 cells and expressed as fold-change compared to untreated control (B). Total RNA was extracted, reverse-transcribed and analyzed by real-time RT-PCR for *Xbp1* (C), *Bip* (E), *Erp72* (F), *Fkbp11* (G), *Grp94* (H), *Edem1* (I), *Chop* (J) and *Trib3* (K). D: *Xbp1* splicing was analyzed and expressed as described in Fig. 1. All results are mean±SEM determined from at least three experiments; **p*<0.05, ***p*<0.01, ****p*<0.001 cytokine effect in each group; †*p*<0.05, ††*p*<0.01, †††*p*<0.001 JNKi effect in each treatment group.

Figure 8. Effect of JNK inhibition on the changes in UPR gene expression in *db/db* mouse islets. Islets isolated from diabetic *db/db* and litter-mate control mice were cultured in the absence (control, *white bars*; and *db/db*, *black bars*) or presence (*db/db*, *striped bars*) of the JNK inhibitor (JNKi, 20 µmol/l) for 24 h. Total RNA was extracted, reverse-transcribed and analyzed by real-time RT-PCR for *Xbp1* (A), *Bip* (C), *Erp72* (D), *Fkbp11* (E), *Grp94* (F), *Edem1* (G), *Chop* (H) and *Trib3* (I). B: *Xbp1* splicing was analyzed and expressed as described in Fig. 1. All results are mean±SEM determined from at least three experiments; **p*<0.05, ***p*<0.01, ****p*<0.001 genotype effect; †*p*<0.05, ††*p*<0.01, †††*p*<0.001 4µ8c treatment effect in d*b/db* islets.

Supplementary Figure 1. Changes in *Xbp1* mRNA expression in islets of diabetes-prone *db/db* and diabetes-resistant *ob/ob* mice at 6 and 16 weeks of age. Islets were isolated from 10 C57BL/KsJ control and 8 pre-diabetic *db/db* mice at 6 weeks of age, 15 C57BL/KsJ control and 12 diabetic *db/db* mice at 16 weeks of age, 6 C57BL/6J control and 5 *ob/ob* mice at 6 weeks of age, and 5 C57BL/6J control and 7 *ob/ob* mice at 16 weeks of age. Total RNA was extracted, reverse-transcribed and analyzed by real-time RT-PCR. mRNA levels were expressed as fold-change of the levels in respective age-matched controls (represented by the dashed line). Shown are changes in islets of *db/db* and *ob/ob* mice at 6 (*white bars*) and 16 (*black bars*) weeks of age. All results are mean±SEM; **p*<0.05, ***p*<0.01, ****p*<0.001 genotype effect in each age group.

Figure 1

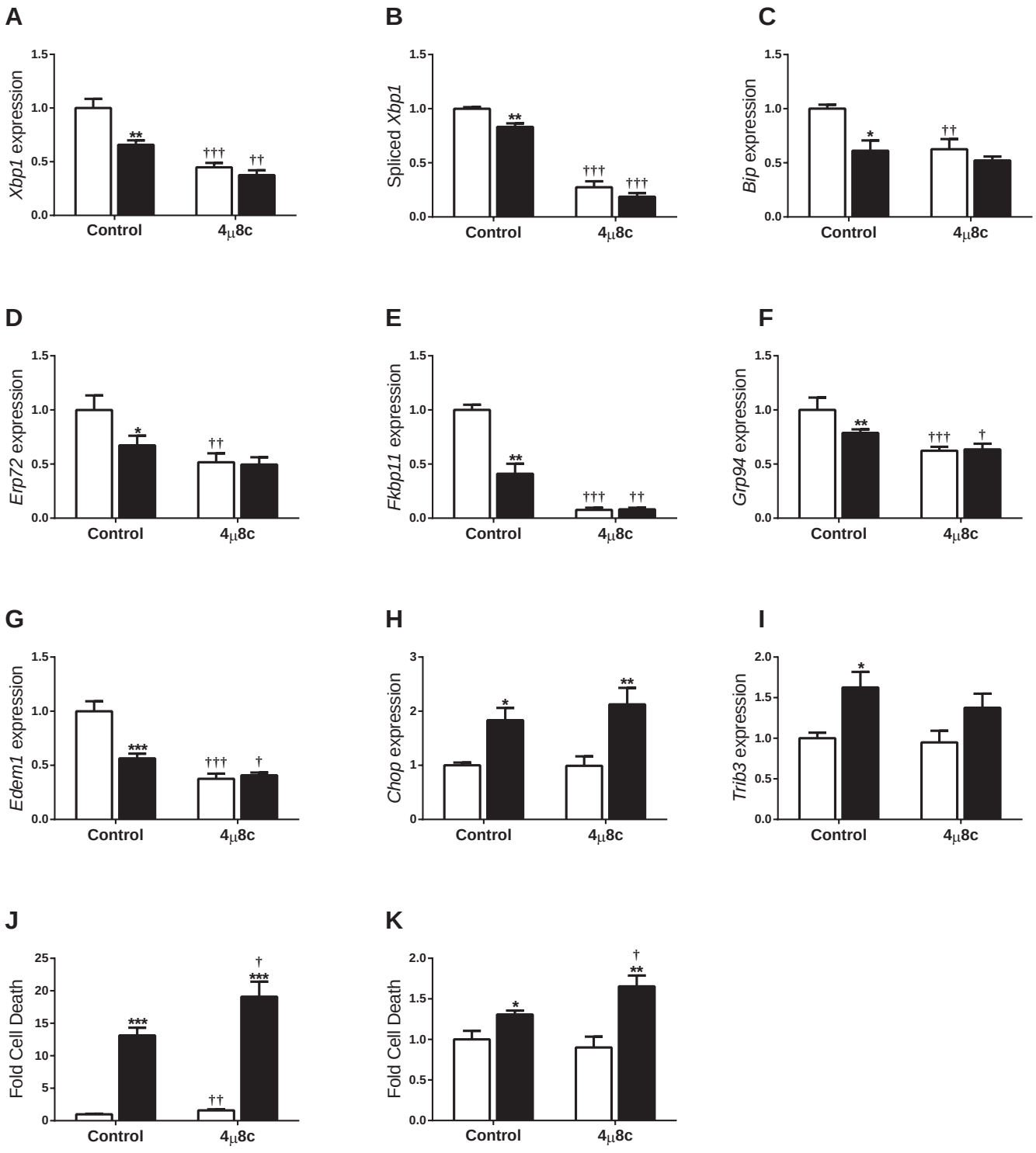
A
Xbp1 expression
1.5
1.0
0.5
0.0
**
†††
††
Control
4μ8c
B
Spliced Xbp1
**
†††
†††
C
Bip expression
*
††
D
Erp72 expression
*
††
E
Fkbp11 expression
**
†††
††
F
Grp94 expression
**
†††
†
G
Edem1 expression
***
†††
†
H
Chop expression
3
2
1
0
*
**
I
Trib3 expression
2.0
1.5
1.0
0.5
0.0
*
J
Fold Cell Death
25
20
15
10
5
0
***
†
***
††
K
Fold Cell Death
2.0
1.5
1.0
0.5
0.0
*
†
**

Figure 2

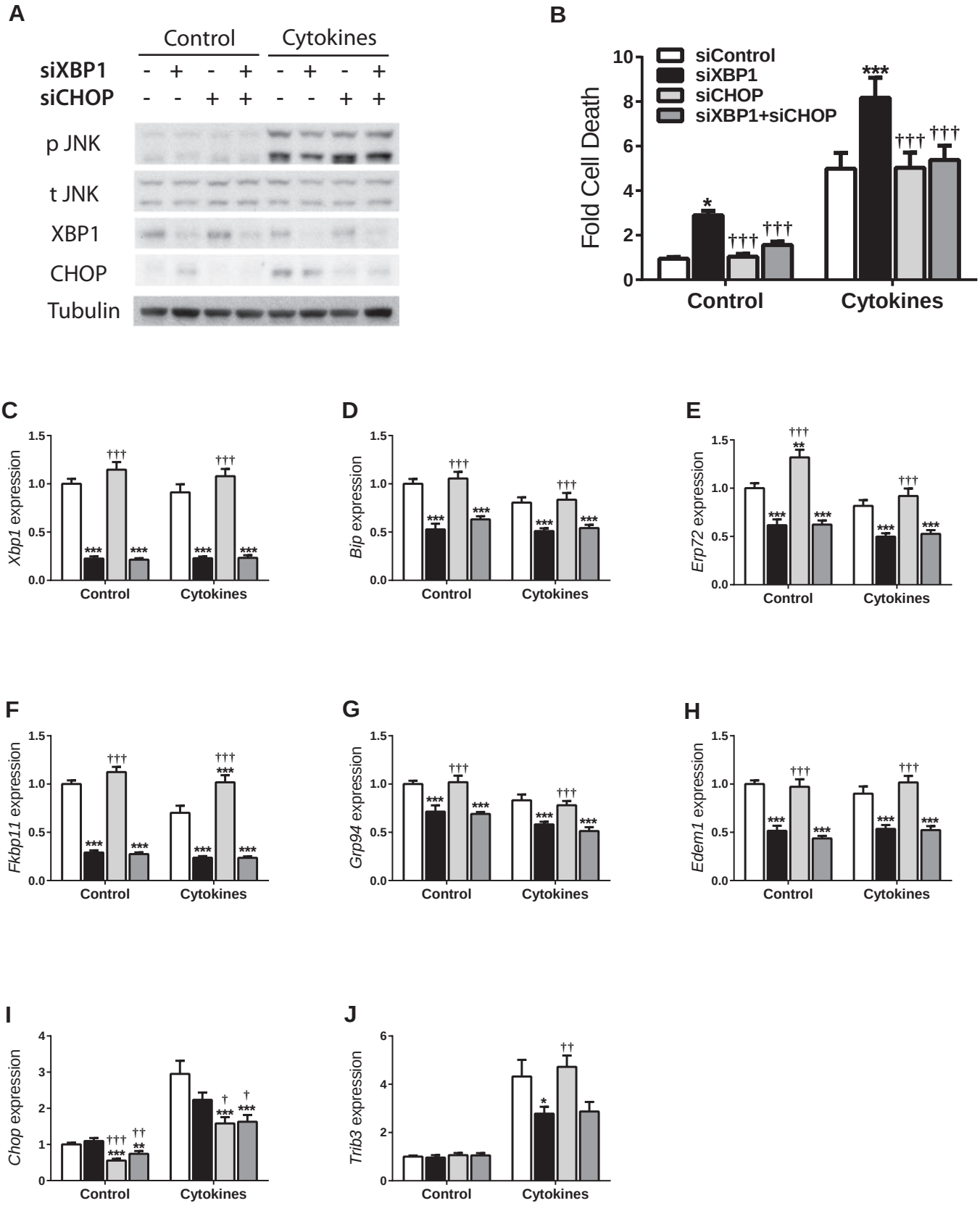
A
Control
Cytokines
siXBP1 - + - + - + - +
siCHOP - - + + - - + +
p JNK
t JNK
XBP1
CHOP
Tubulin
B
siControl
siXBP1
siCHOP
siXBP1+siCHOP
Fold Cell Death
Control
Cytokines
C
Xbp1 expression
D
Bip expression
E
Erp72 expression
F
Fkbp11 expression
G
Grp94 expression
H
Edem1 expression
I
Chop expression
J
Trib3 expression

Figure 3

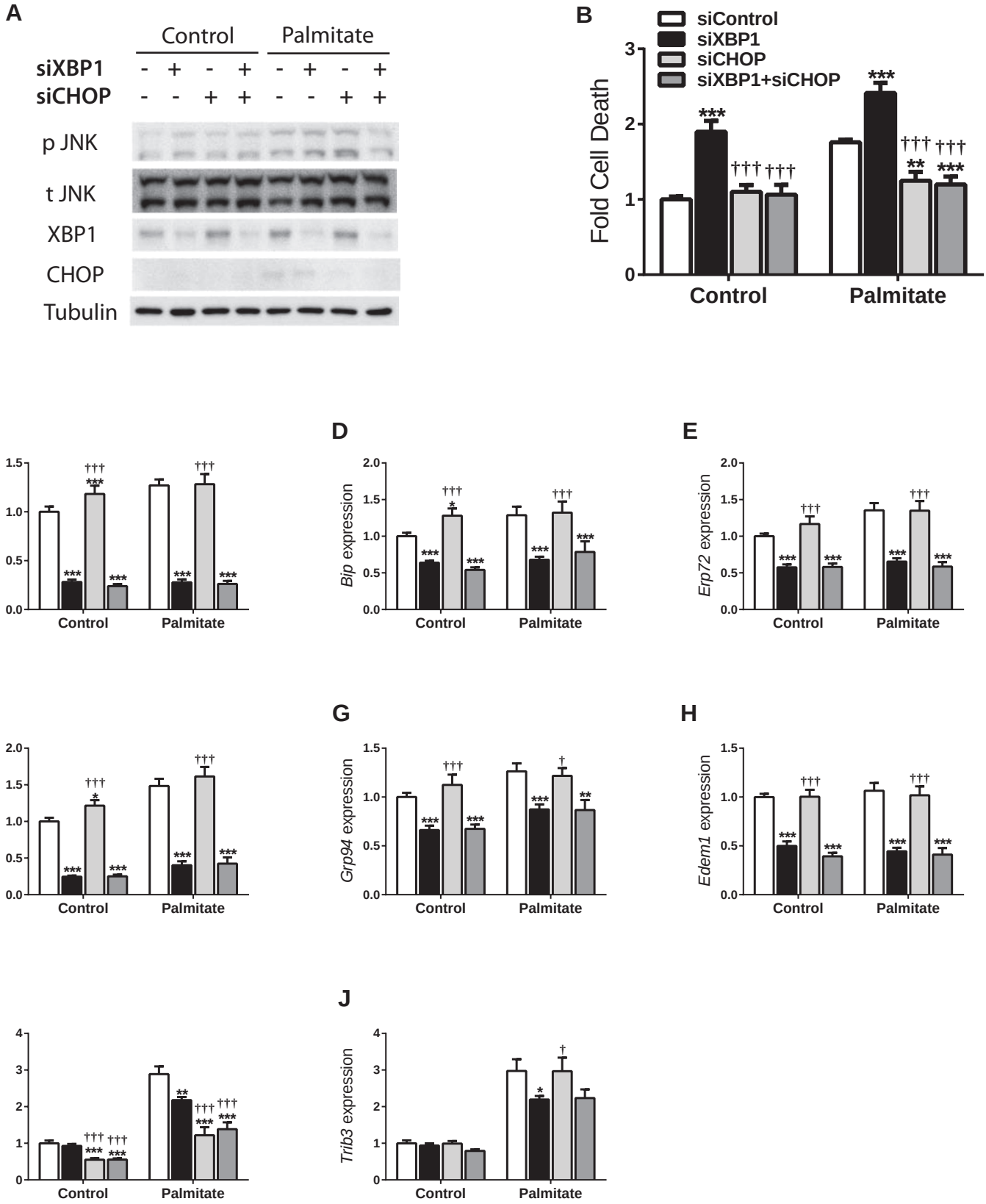
A
Control
Palmitate
siXBP1 - + - + - + - +
siCHOP - - + + - - + +
p JNK
t JNK
XBP1
CHOP
Tubulin
B
siControl
siXBP1
siCHOP
siXBP1+siCHOP
Fold Cell Death
Control
Palmitate
C
Xbp1 expression
D
Bip expression
E
Erp72 expression
F
Fkbp11 expression
G
Grp94 expression
H
Edem1 expression
I
Chop expression
J
Trib3 expression

Figure 4

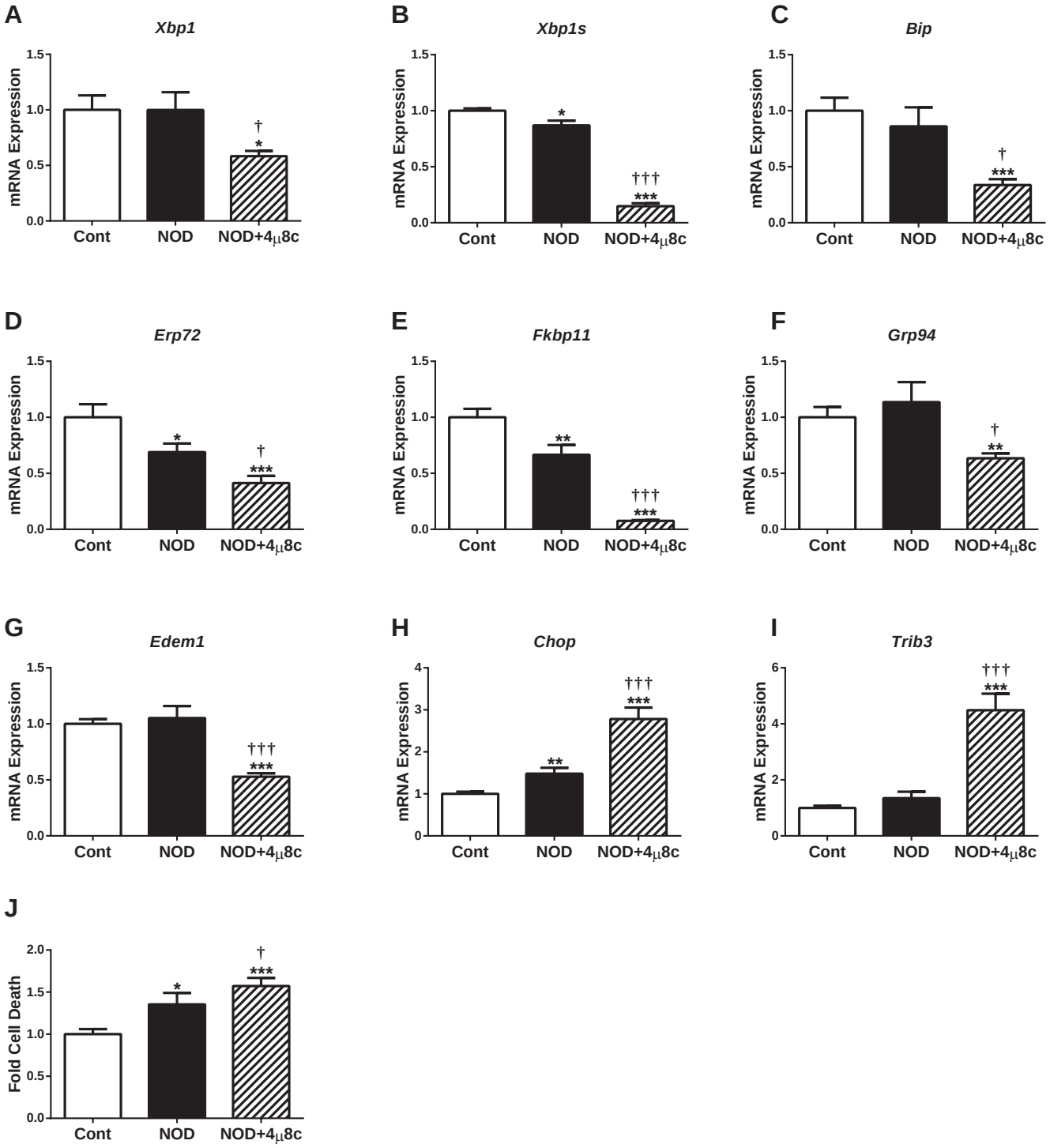
A
Xbp1
mRNA Expression
1.5
1.0
0.5
0.0
†
*
Cont
NOD
NOD+4μ8c
B
Xbp1s
mRNA Expression
*
†††
***
C
Bip
mRNA Expression
†
***
D
Erp72
mRNA Expression
*
†
***
E
Fkbp11
mRNA Expression
**
†††
***
F
Grp94
mRNA Expression
†
**
G
Edem1
mRNA Expression
†††
***
H
Chop
mRNA Expression
4
3
2
1
0
**
†††
***
I
Trib3
mRNA Expression
6
4
2
0
†††
***
J
Fold Cell Death
2.0
1.5
1.0
0.5
0.0
*
†
***

Figure 5

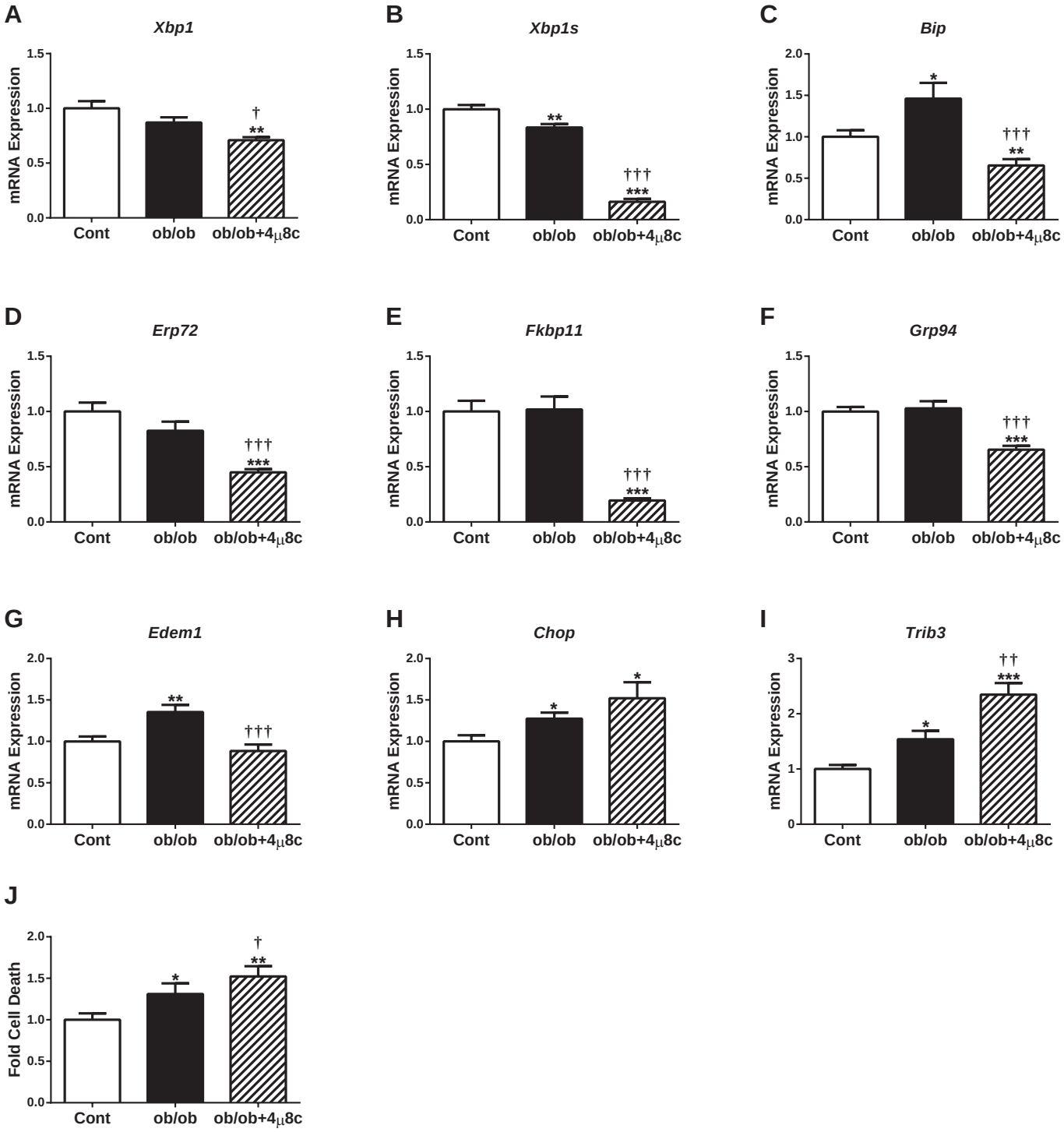
A
Xbp1
mRNA Expression
1.5
1.0
0.5
0.0
†
**
Cont
ob/ob
ob/ob+4μ8c
B
Xbp1s
mRNA Expression
1.5
1.0
0.5
0.0
**
†††
***
Cont
ob/ob
ob/ob+4μ8c
C
Bip
mRNA Expression
2.0
1.5
1.0
0.5
0.0
*
†††
**
Cont
ob/ob
ob/ob+4μ8c
D
Erp72
mRNA Expression
1.5
1.0
0.5
0.0
†††
***
Cont
ob/ob
ob/ob+4μ8c
E
Fkbp11
mRNA Expression
1.5
1.0
0.5
0.0
†††
***
Cont
ob/ob
ob/ob+4μ8c
F
Grp94
mRNA Expression
1.5
1.0
0.5
0.0
†††
***
Cont
ob/ob
ob/ob+4μ8c
G
Edem1
mRNA Expression
2.0
1.5
1.0
0.5
0.0
**
†††
Cont
ob/ob
ob/ob+4μ8c
H
Chop
mRNA Expression
2.0
1.5
1.0
0.5
0.0
*
*
Cont
ob/ob
ob/ob+4μ8c
I
Trib3
mRNA Expression
3
2
1
0
*
††
***
Cont
ob/ob
ob/ob+4μ8c
J
Fold Cell Death
2.0
1.5
1.0
0.5
0.0
*
†
**
Cont
ob/ob
ob/ob+4μ8c

Figure 6

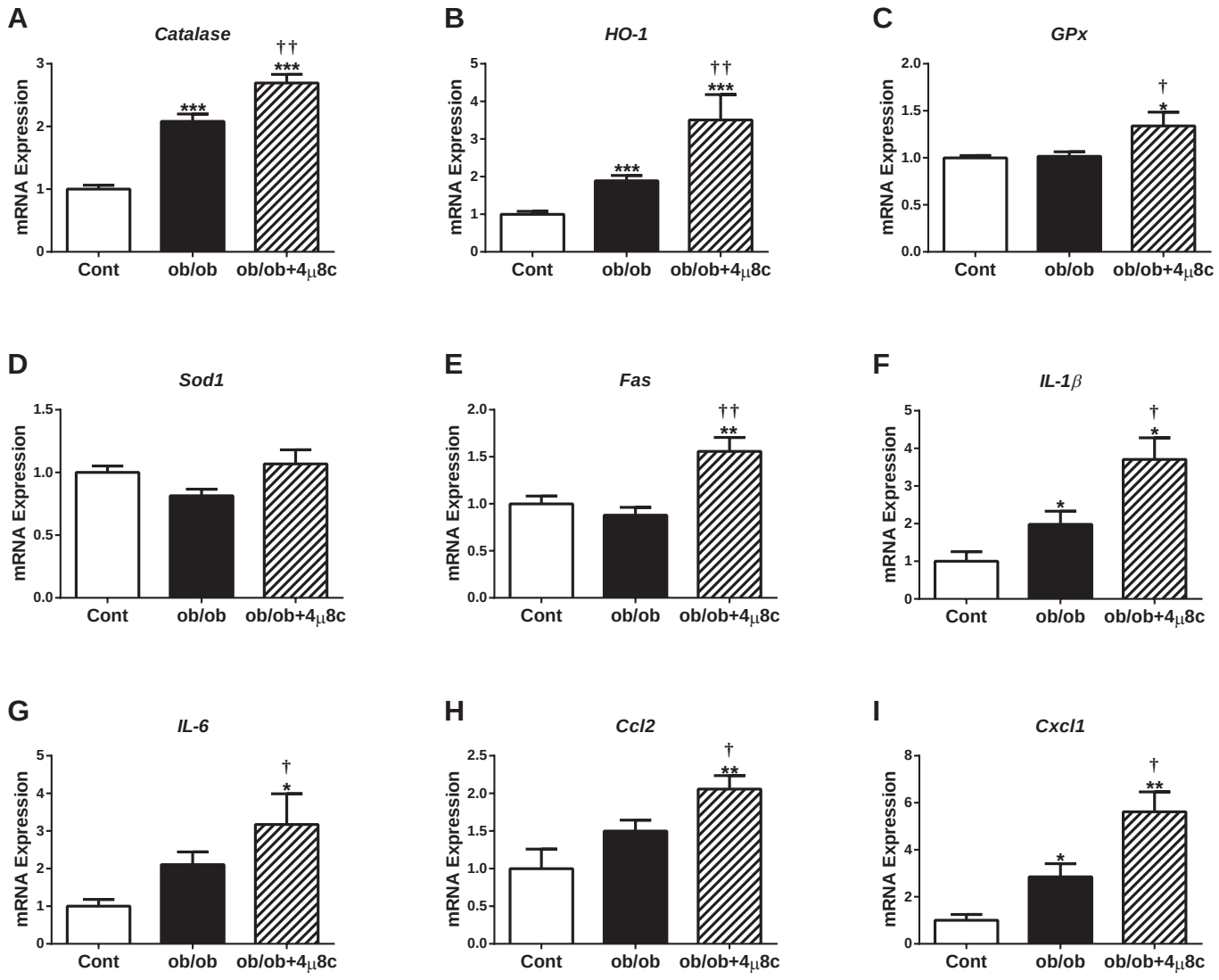
A
Catalase
mRNA Expression
Cont
ob/ob
ob/ob+4μ8c
B
HO-1
C
GPx
D
Sod1
E
Fas
F
IL-1β
G
IL-6
H
Ccl2
I
Cxcl1

Figure 7

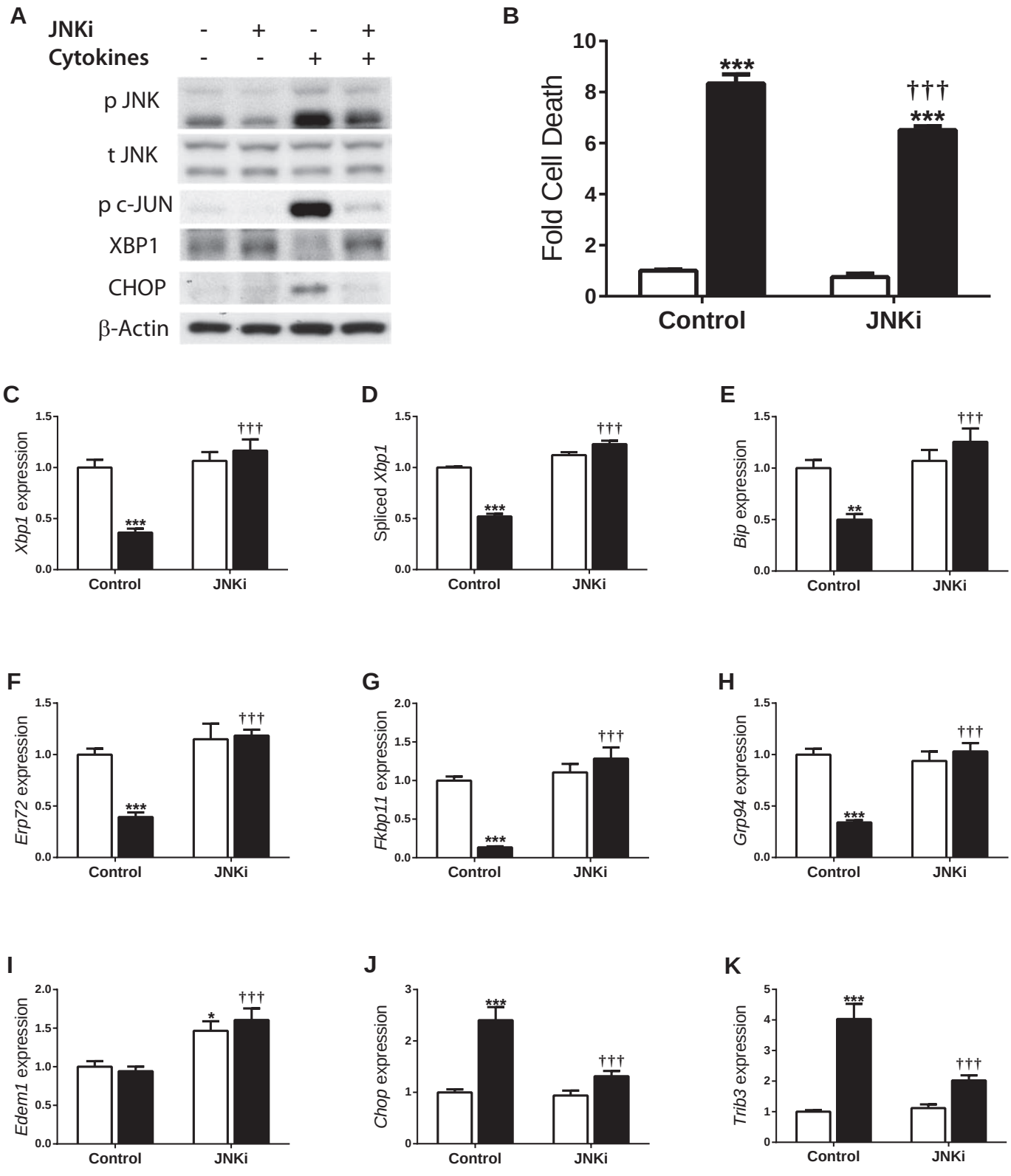
A
JNKi - + - +
Cytokines - - + +
p JNK
t JNK
p c-JUN
XBP1
CHOP
β-Actin
B
Fold Cell Death
Control
JNKi
C
Xbp1 expression
D
Spliced Xbp1
E
Bip expression
F
Erp72 expression
G
Fkbp11 expression
H
Grp94 expression
I
Edem1 expression
J
Chop expression
K
Trib3 expression

Figure 8

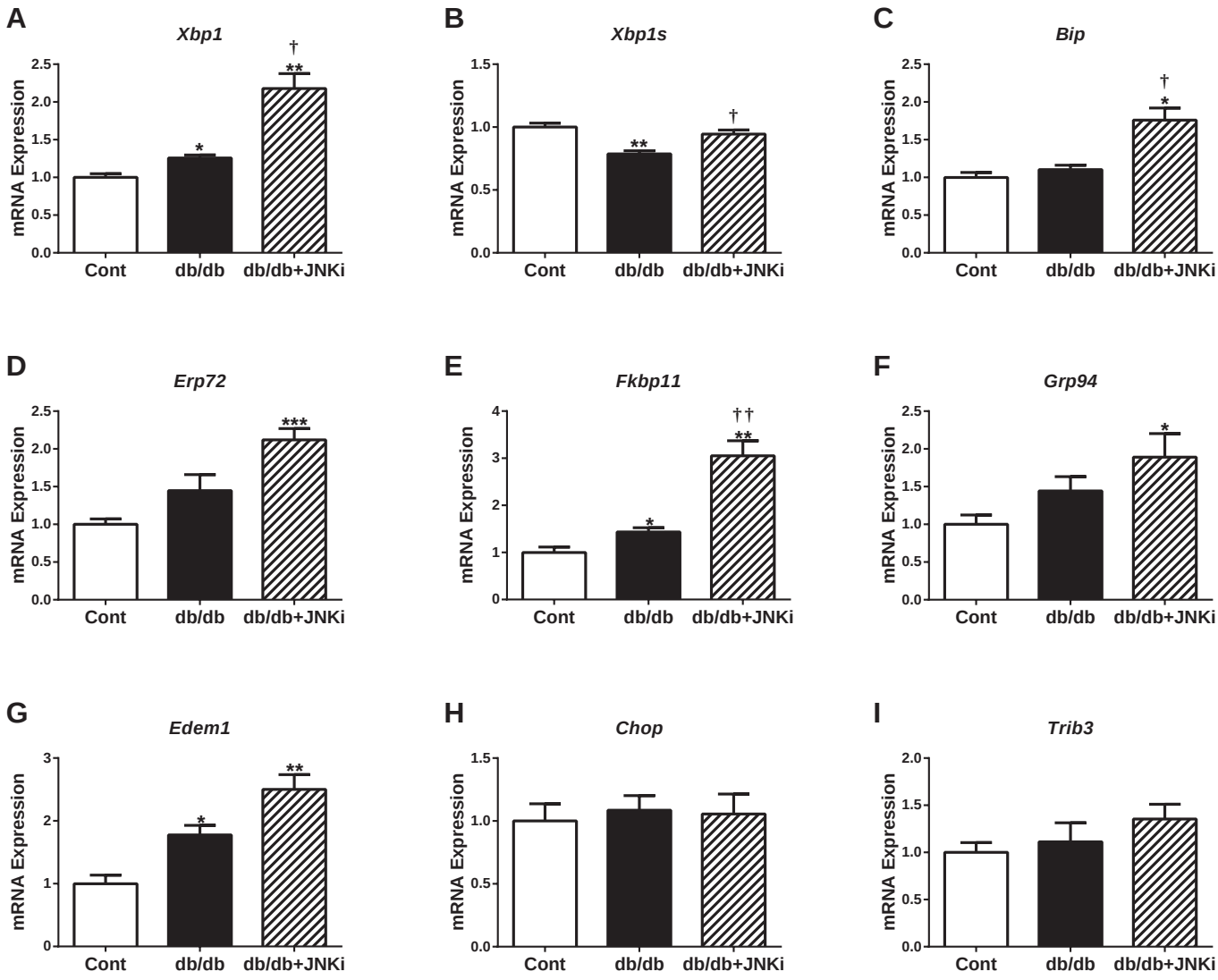
A
Xbp1
mRNA Expression
Cont
db/db
db/db+JNKi
B
Xbp1s
C
Bip
D
Erp72
E
Fkbp11
F
Grp94
G
Edem1
H
Chop
I
Trib3

Supplementary Figure 1

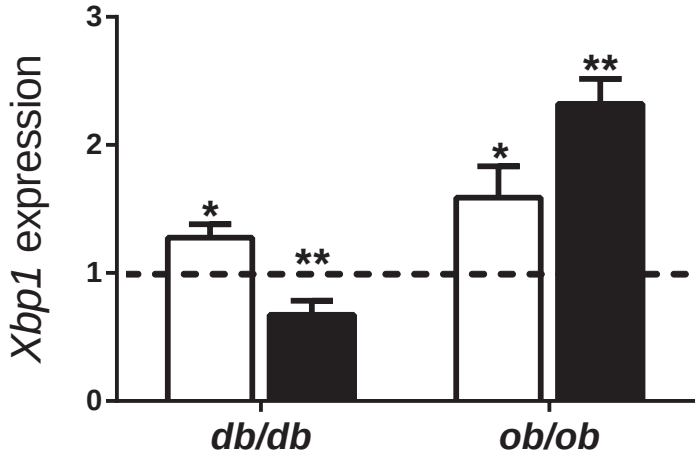

SUPPLEMENTARY DATA

Supplementary Table S1. Sequences of oligonucleotide primers

Gene symbol	5' Oligonucleotide	3' Oligonucleotide
Bip (Hspa5, Grp78)	AGGACAAGAAGGAGGATGTGGG	ACCGAAGGGTCATTCCAAGTG
Catalase	ATGAAGCAGTGGAAGGAGCAGC	CTGTCAAAGTGTGCCATCTCGTC
Ccl2 (Mcp-1)	CCACTCACCTGCTGCTACTCATTC	TCTGGACCCATTCCTTCTTGG
Chop (Ddit3; Gadd153)	TTCACTACTCTTGACCCTGCGTC	CACTGACCACTCTGTTTCCGTTTC
Cxcl1 (Gro-1)	CAAACCGAAGTCATAGCCACACTC	TTGTCAGAAGCCAGCGTTCAC
Cyclophilin A	TGTGCCAGGGTGGTGACTTTAC	TGGGAACCGTTTGTGTTTGG
Edem1	GCAATGAAGGAGAAGGAGACCC	TAGAAGGCGTGTAGGCAGATGG
Erp72 (Pdia4)	AGTCAAGGTGGTGGTGGGAAAG	TGGGAGCAAAATAGATGGTAGGG
Fas	AACCAGACTTCTACTGCGATTCTCC	CCTTTTCCAGCACTTTCTTTTCCG
Fkbp11	ACACGCTCCACATACACTACACGG	ATGACTGCTCTTCGCTTCTCTCCC
GPx (GPx-1, CGPx)	ACAGTCCACCGTGTATGCCTTC	CTCTTCATTCTTGCCATTCTCCTG
Grp94 (Hsp90b1)	AAACGGCAACACTTCGGTCAG	GCATCCATCTCTTCTCCCTCATC
HO-1 (Hmox1, Hsp32)	CCACACAGCACTATGTAAAGCGTC	GTTCGGGAAGGTAAAAAAAGCC
IL-1β	TGTTCTTTGAAGTTGACGGACCC	CCACAGCCACAATGAGTGATACTG
IL-6	CAAGAGACTTCCATCCAGTTGCC	CATTTCCACGATTTCCCAGAGAAC
Sod1 (Cu/ZnSOD)	ATGGGGACAATACACAAGGCTG	CAATGATGGAATGCTCTCCTGAG
Trib3	TCTTCAGCAACTGTGAGAGGACG	TCCAGACATCAGCCGCTTTG
Xbp1	GCAGCAAGTGGTGGATTTGG	AGATGTTCTGGGGAGGTGACAAC
Xbp1 (Splicing)	AAACAGAGTAGCAGCGCAGACTGC	GGATCTCTAAAACTAGAGGCTTGGTG

Aliases of gene symbols given in parentheses